Numerical Characterization of the Performance Curve of a Regenerative Pump-as-Turbine

NUMERICAL CHARACTERIZATION OF THE PERFORMANCE CURVE OF A REGENERATIVE PUMP-AS-TURBINE

Giulio Cantini
Dipartimento di Ingegneria Industriale (DIEF), Università di Firenze
Via di Santa Marta, 3 – 50142, Firenze, Italia
giulio.cantini@unifi.it

Simone Salvadori[1]
Dipartimento Energia (DENERG), Politecnico di Torino
Corso Duca degli Abruzzi, 24 – 10129 Torino, Italia
simone.salvadori@polito.it

ABSTRACT

Energy companies in the power generation field are continuously searching for green technologies to reduce pollutant emissions. In that context, small hydropower plants represent an attractive solution for distributed electricity generation. Reverse-running centrifugal pumps (also known as “pump-as-turbines”, PaT) are increasingly selected in that field. Amongst the existing type of pumps, drag-type regenerative pumps (RP) can perform similarly to radial centrifugal pumps in terms of head and efficiency for low specific speed values. For a fixed rotational speed, RPs with linear blades work as pump or turbine only depending on the flow rate. Such peculiarity makes it particularly intriguing to evaluate RPs working characteristic in the turbine operating mode. In the present paper, the performance of three Regenerative Pump-as-Turbines (RPaT) are analyzed using Computational Fluid Dynamics (CFD). The numerical approach is validated

[1] Corresponding author.

using experimental data for both an RP (in the pump working region) and a regenerative turbine (RT) (in the turbine working region). Finally, the numerical simulation of a small-scale RP allows for characterizing both the pump and the turbine regions. Results shows that for a RPaT it is possible to find a “switch region” where the machine turns from behaving as a pump to behaving as a turbine, the losses not being overcome by the turbine power output. The analysis of the RPaT also shows the inversion of the flow pattern and the constant positioning of the pivot around which the flow creates the typical helical structure that characterizes RPs.

INTRODUCTION

Recent changes in the power generation field oblige energy companies to move towards the development of small hydropower plants for distributed electricity generation. Although the most logical solution would be the selection of a radial turbine for those plants, reverse-running centrifugal pumps (also known as “pump-as-turbines”, PaT) are increasingly selected to generate and recover power thanks to their simplicity and reduced costs (if compared with turbines).

Amongst the existing type of pumps, drag-type regenerative pumps (RPs) combine the high pressure rise of positive displacement pumps with the flexible operation of centrifugal pumps. They are usually considered as an alternative to purely radial solutions since they are characterized by low specific speed values. In that range of application, RPs can substitute purge and water/oil pumps (in the automotive field) as well as components in a refrigeration cycle for distributed air conditioning (e.g., for a train coach). Their main drawback is represented by a lower peak efficiency with respect to centrifugal

turbomachines over a wide range of operating conditions. However, in the optimal range of application, regenerative machines represent a compact solution that guarantees remarkable performance at a lower rotational speed with respect to centrifugal pumps.

RPs are characterized by the presence of an impeller and of a side channel. The flow enters the impeller at the lower radius and is energized while passing through the blade channel. It is hence purged towards the side channel at a higher radius, thus reducing its velocity along a helical trajectory and increasing the pressure level. Considering that each particle is subjected to several complete helical trajectories, RPs are intrinsically multistage machines.

Wilson *et al.* [1] demonstrated that the efficiency of regenerative pumps is limited by incidence losses, hydraulic losses and by inlet/outlet losses. Furthermore, high dependence from the dimension of leakages has been demonstrated by Cantini *et al.* [2]. Karassik *et al.* [3] underlined that RPs guarantee a higher upper limit of pressure rise with respect to centrifugal and rotary machines at lower capacity values. Brown [4] concluded that, except for power absorption, RPs are superior to centrifugal pumps (at least in the chemical engineering field).

It is possible to distinguish two categories of RPs. The “aero-foil blades” group includes all the regenerative pumps whose impeller shows a C-shaped side channel (see Sixsmith and Altmann [5] and Griffini *et al.* [6]). The “plane blades” group is characterized by a geometry where the flow moves almost unguided through the impeller and the side channel does not provide any guidance to the circulatory flow (see Yoo *et al.* [7][8], Badami *et al.* [9]

and Insinna *et al.* [10]). The “plane blades” solution is preferable when low flow rate and compactness are requested, which is the case analyzed in the present work.

Regenerative turbines (RTs) represent the counterpart of RPs in the energy harvesting field. RTs share with RPs both the geometrical characteristics and the working principle, being the fluid driven to move along a helical trajectory to recover energy from an external source. Although RTs are characterized by good performance at low specific speed, the higher efficiency of centripetal turbines has limited their usage in power systems. Anyway, it must be underlined that RTs are able to deal with two-phase flows, are almost noiseless and are compact and reliable machines. Therefore, their use in small-scale power plants based on the organic Rankine cycle (ORC) can be considered.

Due to the limited usage of RTs, both scientific and industrial research about in- and off-design performance is almost negligible. The contributions by Balje [11][12] represent the most notable exception to this scenario. In fact, Baljé extensively describes the RTs performance as a function of geometrical (area ratio, clearance dimension, blade angle, specific diameter), fluid dynamic (Mach and Reynolds number) and working parameters (pressure and velocity ratio), also proposing diagrams for the optimal selection of the RT.

In a research work by Bartolini and Salvi [13], RTs are experimentally analyzed in the field of decompression of natural gas. The authors aim at increasing the RT performance by modifying the stripper, burnishing the rotor, chamfering the turbine blades, introducing a fin in the peripheral channel, and finally changing the orientation of the intake entrance. For each modification it is possible to track the changes in the mass-flow and the enthalpy variation values, thus identifying the impact of each modification on the RT performance.

The same geometry from Bartolini and Salvi [13] has been recently analyzed by Moradi *et al.* [14] using Computational Fluid Dynamic (CFD) techniques. The numerical setup is initially validated using the available experimental data and then the same configuration is studied at higher temperature ranges. The final aim is to demonstrate that CFD is a reliable tool for the analysis and the optimization of RTs for future application in small-scale ORC plants or cryogenic systems.

It has been previously underlined that RPs and RTs with linear blades share the same geometrical characteristics. This means, in principle, that each RP can be used as a RT by simply changing the working conditions. In fact, contrary to what happens for centrifugal machines, regenerative machines do not require the inversion of the rotational speed and of the inlet/outlet channels. As the present paper will explain by using a widely accepted model for the calculation of the circulatory velocity in RPs, regenerative machines work as pumps for flow coefficients below unity and as turbines for flow coefficients above unity (with some important limitations in the switching region). Therefore, by increasing the flow rate it is possible to switch from a pump to a turbine without any other action to be performed. In those machines, inlet and outlet channels are the same in the forward and in the reverse-running conditions: that peculiarity makes it particularly intriguing to evaluate RPs working characteristic as turbines.

In the authors' opinion, regenerative pumps-as-turbines (RPaTs) will have interesting applications in hydropower plants, in the energy storage field for small-scale power plants and in the refrigeration field. Unfortunately, to the best authors' knowledge there are no information about the performance of a RPaT from pump to turbine regimes in the

scientific literature. Therefore, the aim of this work is to perform a theoretical study of the switching condition between pump and turbine and to hence perform the numerical simulation of an already analyzed RP to extend its performance curve in the turbine region for different rotational speeds.

The present paper is divided into three main sections. In the first part, the theory proposed by Yoo *et al.* [7][8] is extended to take into consideration the fact that a RP can act also as a RT in a different range of flow rates. In the second part, a numerical methodology used to study regenerative turbomachines (both pumps and turbines) is validated using the experimental data from the papers by Yoo *et al.* [7] and by Bartolini and Salvi [13]. In the third part, the same numerical approach is used to perform a numerical campaign aiming at describing the performance (both as pump and as turbine) of a regenerative turbomachine developed at the Department of Industrial Engineering (DIEF) of the University of Florence in cooperation with Pierburg Pump Technology Italy (PPTI) SPA. Results are discussed and conclusions about the possible usage of RPaTs are drawn.

THEORY FOR REGENERATIVE PUMP AS TURBINE

Simplified models are widely used in the preliminary design phase of several machines and components (see for example [15][16][17]). Recently, a 1D model used for performance prediction of RPs has been developed by the Turbomachinery and Combustion Research (TCR) group of the Department of Industrial Engineering (DIEF) of the University of Florence (Italy) with the support of the Modeling R&D Department of Pierburg Pump Technology. The development and validation of the DART (Design and

Analysis tool for Regenerative Turbomachinery) code, which is based on the theory developed by Yoo *et al.* [7][8] with some modifications concerning the calculation of hydraulic losses and leakage flows is described in Insinna *et al.* [10] and in Cantini *et al.* [2].

To better understand the performance of a RP when working as a RT, the model by Yoo *et al.* [7] for the circulatory velocity is analyzed under some assumptions. That model links the pressure rise with the evolution of circulatory velocity along tangential direction. For the sake of brevity, a complete definition of the variables used in the present work can be found in the abovementioned papers by Yoo *et al.* [7] and Insinna *et al.* [10].

Equation (1) allows for the calculation of the head:

$$gH = \vartheta \frac{Q_c(\theta_{out})}{Q_s}(\sigma U_e^2 - \alpha U_i^2) - \Delta gH_\theta - \Delta gH_{in} - \Delta gH_{out} \quad (1)$$

The circulatory flow rate $Q_c(\theta)$ is a function of the tangential position and is defined as in Equation (2):

$$Q_c(\theta) = \int_{\theta_{in}}^{\theta} A_c V_c(\varepsilon) d\varepsilon \quad (2)$$

The sweeping flow rate Q_s is equal to the volume swept in the side channel per unit time at the rotational speed of the impeller and is calculated as reported in Equation (3):

$$Q_s = A_o r_{g,o} \Omega \tag{3}$$

Still referring to Equation (1), U_e is the impeller tangential velocity at the mean flow exit radius and U_i is the impeller tangential velocity at the mean flow inlet radius, σ is the slip factor and α is the incidence factor. The working condition of the machine is reduced to calculate $V_c(\theta)$, which can be obtained by resolving a non-linear differential equation derived from the balance of energy and momentum of momentum (Equation (4)):

$$\frac{dV_c}{d\theta} = \frac{A_c}{(Q + Q_v)}\left(C_3 + C_2 V_c - C_1 {V_c}^2\right) \tag{4}$$

In Equation (4), Q_v is the flow rate equal to the volume swept in the vanes per unit time at the rotational speed of the impeller. The coefficients C_1, C_2 and C_3 are defined as follows:

$$C_1 = \frac{B_c}{2} + \frac{\vartheta}{2}\left(\frac{A_c \tan(\beta_{opt})}{(r_c - r_0) r_i}\right)^2 \tag{5}$$

$$C_2 = \frac{\vartheta(1-\alpha) U_i A_c \tan(\beta_{opt})}{(r_c - r_0) r_i} \tag{6}$$

$$C_3 = \vartheta(\sigma U_e^2 - \alpha U_i^2)(1-\varphi) - \frac{\vartheta(1-\alpha)^2 {U_i}^2}{2} \tag{7}$$

The present theory for RPs can be extended to study RTs after some modifications. In fact, the equations need to be changed considering the different pattern of circulatory velocity. In RPs, the fluid enters at the lower section of the blade and moves out from the blade at the upper section while in RTs the fluid performs the exact opposite trajectory, entering at the blade tip and exiting near the hub. The equations obtained by Yoo *et al.* [7] for the pump case are based on a positive value for the circulatory velocity, whereas for turbines the circulatory velocity is to be considered as negative. The equations will hence change as follows:

- U_e is the velocity of the impeller nearby the tip of the blade in the pump case and nearby the hub of the blade in the turbine case;
- U_i is the velocity of the impeller nearby the hub of the blade in the pump case and nearby the tip of the blade in the turbine case;
- the changes in the value of the slip factor depend on the method used for its calculation.

If the C_i parameters are constant along the tangential coordinate (i.e., $\frac{dC_i}{d\theta} = 0$), an analytical solution of Equation (4) can be found. First, a particular constant solution $V_c = K$ is to be found; substituting K into the brackets of Equation (4) Equation (8) is obtained, thus allowing for the computation of K using Equation (9):

$$C_3 + C_2 K - C_1 K^2 = 0 \tag{8}$$

$$K = \frac{C_2 + \sqrt{C_2^2 + 4C_1 C_3}}{2C_1} \tag{9}$$

Once K has been found, the general solution must be searched in the form $V_c = K + \frac{1}{z(\theta)}$. By substituting this term into Equation (4), the final form for the V_c expression is reported in Equation (10):

$$V_c = K + \frac{1}{S\ exp[\Gamma(2C_1 K - C_2)\theta] + \frac{C_1}{C_2 - 2C_1 K}} \tag{10}$$

The term Γ is defined as $\Gamma = \frac{A_c}{(Q+Q_v)}$ whereas S is a constant that can be obtained from the boundary conditions (i.e., from the value of circulatory velocity nearby the inlet $V_c(\theta_{in})$). A typical evolution of the circulatory velocity along the peripheral coordinate (excluding the stripper region) is reported in Figure 1 for a small-scale RP. For the case in which the machine works as a turbine, the plot results to be similar with the notable difference that the circulatory velocity V_c will only assume negative values. Note that if $V_c(\theta_{in}) < K$, then K is the maximum magnitude of the circulatory velocity.

Once V_c is obtained from Equation (10), Q_c and gH can be obtained from Equations (1) and (2). It must be underlined that, to establish a circulatory velocity pattern, the solution

needs to be a real function ($V_c: \mathbb{R} \rightarrow \mathbb{R}$). This implies that $K \in \mathbb{R}$. Therefore, the discriminant of Equation (8) must be positive:

$$C_2^2 + 4C_1C_3 \geq 0 \tag{11}$$

A simplified solution can be obtained for purely radial vanes (which characterize most peripheral pumps). In fact, in those cases $\tan(\beta_{opt}) = 0$ and then the equations simplify down. In particular, $C_2 = 0$ and the condition for the existence of a real solution from Equation (11) is that $C_3 \geq 0$. In conclusion, a regenerative machine works as a pump if the condition reported in Equation (12) is satisfied:

$$\varphi < 1 - \frac{(1-\alpha)^2 U_i^2}{2(\sigma U_e^2 - \alpha U_i^2)} = 1 - \delta_1 \tag{12}$$

On the contrary, it works as a turbine if the condition in Equation (13) is satisfied:

$$\varphi > 1 - \frac{(1-\alpha)^2 U_i^2}{2(\sigma U_e^2 - \alpha U_i^2)} = 1 + \delta_2 \tag{13}$$

The main difference between Equations (12) and (13) is that the term $(\sigma U_e^2 - \alpha U_i^2)$ changes its sign (negative for turbines, positive for pumps). Therefore, for machines equipped with radial vanes there is always an interval $\varphi \in (1 - \delta_1, 1 + \delta_2)$ where the regenerative machine does not work. As demonstrated by the RPaT performance curves

obtained for the PPTI machine and discussed in another section, the reason why a non-working region arises is because as the regenerative machine tends to work as a turbine the power output might still not be enough to overcome the hydraulic losses. The extension of the switch interval is wider than the theoretical one given that inflow and outflow losses are not included in the simplified model. It can also be noticed that, neglecting all the losses, the behavior of the machine is simply defined by the flow rate:

- if $\varphi < 1 - \delta_1$ the machine works as a pump because the circulatory velocity is lower than the blades' tangential velocity (essentially, the fluid is "dragged" by the blades);
- if $\varphi > 1 + \delta_2$ the machine works as a turbine because the circulatory velocity is higher than the blades' tangential velocity (the impeller moves thanks to the energy transferred from the fluid).

An example of what is expected to happen in a regenerative machine in terms of velocity triangles when switching between pump and turbine is reported in Figure 2. In a RP, the tangential component of the absolute velocity V_{abs} is lower than the entrainment velocity Ωr_{hub} at its inlet section (close to the hub), while in a RT the same component is higher than Ωr_{tip}. It is worth underlining that a regenerative machine has two different Best Efficiency Points (BEPs) in terms of incidence losses (see dashed vectors in Figure 2): the first one at a lower flow rate ($\varphi < 1 - \delta_1$) characterizes the RP and the second one ($\varphi > 1 + \delta_2$) is the one of the RT. Therefore, the BEPs of a regenerative machine depend on the blade height, on the rotational velocity and on the blade lean. For the sake of simplicity,

the analysis performed in the present work is limited to machines characterized by purely radial blades.

SETUP OF THE NUMERICAL SIMULATIONS

In the present paper, three different regenerative machines are analyzed using CFD simulations. Two of them (the RP by Yoo *et al.* [7] and the RT by Bartolini and Salvi [13]) are used for validation purposes. Therefore, all the numerical simulations share the same setup described in the present section. Major changes (i.e., the number of elements of the final mesh and the average y^+ value) are underlined in the appropriate sections.

The computational grid used for the simulations of the RP by Yoo *et al.* [7] and of the RT by Bartolini and Salvi [13] is composed by two interfaced, non-conformal sub-domains. The side channel part includes all the stationary elements whereas the impeller region only includes the rotating blades. Due to the complexity of the geometry, a hybrid unstructured grid with prismatic layers at walls and a tetrahedral core is generated with the commercial software CENTAUR™ by Centaursoft. Attention is dedicated to the refinement of the stripper leakage, which is critical for the correct evaluation of both leakage flow and losses. The overall grid resolution is coherent with the one shown by Insinna *et al.* [10] and with the one shown by Moradi *et al.* [14].

The computational grid used for the simulation of the pump described by Insinna *et al.* [10] is composed by the impeller, a porting plate (including the stripper), the remaining part of the side channel and inlet and outlet ducts (no disk clearance is considered). A hybrid unstructured grid, with 20 prismatic layers at wall and tetrahedral core, is generated for the porting plate using the commercial software CENTAUR™ by Centaursoft.

The other modules are discretized by means of multiblock structured grids generated with the commercial software ANSYS® ICEM CFD™. All the necessary interfaces between the modules are non-conformal.

For all the investigated regenerative machines, the inlet and outlet ducts are extended respectively about 6 diameters upstream and about 12 diameters downstream of the pump to avoid the formation of flow recirculation on the outlet section due to the presence of residual swirl under some operating conditions. The final characteristics of all the computational meshes are appropriate to make the problem grid-independent according to the works of Quail *et al.* [19] and Nejadrajabali *et al.* [20].

The numerical campaign is carried out using the ANSYS® Fluent® 2019 R2 solver. A second-order accurate approach in space is used while the SIMPLE algorithm is exploited for pressure-velocity coupling. Following the approach considered in [14], a compressible model (perfect gas) is used for the study of the flow evolving in the RT by Bartolini and Salvi [13]. On the contrary, the flow that develops in the other two cases is considered incompressible, then a constant density value is used.

Steady simulations were performed using the “frozen rotor” approach. The impeller is frozen in a symmetrical position with respect to the stripper, with the maximum closure of this latter by the vanes. This position was chosen to compare the results also with DART’s predictions since such configuration is assumed in the estimation of leakage flows. However, it has been verified by Insinna *el al.* [10] that a change in the relative positioning between the impeller and the static parts does not substantially modify the obtained results for regenerative turbomachines. For the present study, no full unsteady

computation has been performed due to the explorative nature of the research, which is mainly devoted to the evaluation of the performance as turbine of a regenerative machine originally designed as pump.

The realizable k-ε model [21] is used as turbulence closure in conjunction with the Menter-Lechner y^+-independent near-wall treatment [22]. The selected turbulence closure demonstrated to be reliable for the prediction of performance of regenerative pumps, as shown by Quail *et al.* [19].

NUMERICAL SIMULATION OF YOO'S RP [7]

The first regenerative turbomachine that has been considered for the validation of the numerical approach is the "Model 1" pump described by Yoo *et al.* [7]. The same RP has also been used by Insinna *et al.* [10] for the validation of the already cited 1D DART code. Such a RP is characterized by a radial-bladed, "double-sided" impeller (i.e., they consist in two symmetrical sides). The Reynolds number of the machine, referred to the impeller tip velocity and tip diameter, is $3.39 \cdot 10^5$. A set of geometrical details of the RP can be found in Yoo *et al.* [7] whereas some specific information (i.e. blade number and inlet/outlet channels' diameter) has been communicated by the author himself [18].

Due to the geometrical and fluid dynamic symmetry of the present turbomachine, only half of the RP is modelled using CFD. The control volume for the numerical simulation includes inlet and outlet channels, the impeller, the side channel, and the stripper region. The disk clearance between the impeller and the side channel is not considered in the present computation to reduce its complexity. A symmetry plane positioned in the side channel domain is used to mimic the presence of the other half of the turbomachine. The

inlet and outlet channels have been positioned aligned with the machine axis. The numerical setup has also been checked using the most recent version of the DART code [2] that allows for the correct calculation of disk leakage flows and losses.

A front/rear view of the computational mesh is reported in Figure 3. Five prismatic layers with a grow rate of 1. have been used to model the boundary layer on the viscous walls. The final mesh for the side channel (including inlet/outlet channels) contains about $11.9M$ elements whereas the impeller is composed by about $6.3M$ elements. At the maximum simulated flow rate, the average y^+ is about $3.$ in the side channel and $10.$ in the impeller (both compatible with the y^+-independent approach).

The comparison between the experimental data, CFD results and DART's predictions in the pump regime is reported in Figure 4 and Figure 5. The hydraulic efficiency for the pump regime is defined as $\eta = \frac{\rho g H}{P}$ (the inverse for the turbine regime). It is possible to observe that both CFD results and DART's predictions are satisfying. The CFD points at lower flow coefficients (approximately $\varphi = 0.25$ and $\varphi = 0.4$) are very close to the corresponding experimental data. At higher flow rates (approximately $\varphi = 0.5$ and $\varphi = 0.67$), when inlet/outlet losses become relevant, the numerical simulation tends to overestimate the load coefficient (and then to underestimate the hydraulic efficiency) with respect to DART, whereas nothing can be said in comparison with the experimental data that are not available for a flow coefficient higher than $\varphi = 0.5$. No experimental data are available about the flow field (i.e., circulatory velocity at different flow rates), thus making it impossible to further validate the numerical setup. However, the numerical approach can be considered sufficiently accurate in the pump regime.

The performance of Yoo's regenerative pump is also analyzed considering three working conditions characterized by a flow coefficient higher than unity. The data reported in Figure 6 show that, within the investigated range, the load coefficient tends to increase whereas the efficiency curve encounters a maximum and then tends to diminish. Although the absence of any experimental data and the limited amount of CFD data do not allow for more detailed conclusions, it can be underlined that these observations are coherent with what is reported in the following sections for Bartolini's RT and for Pierburg's RP in the turbine range.

NUMERICAL SIMULATION OF BARTOLINI'S RT [13]

The geometry analyzed to validate the present numerical methodology for a RT is the one experimentally studied by Bartolini and Salvi [13] and numerically simulated by Moradi *et al.* [14] for the expansion of natural gas. A complete description of the RT can be found in [14] and a brief description alone will be given here.

The RT is a single-sided machine equipped with semi-circular vanes and by a circular side channel. It is a different solution from the one proposed by Yoo *et al.* [7] and is very similar to the RP designed by Insinna *et al.* [10]. The control volume for the computation includes inlet/outlet channels, impeller, side channel and stripper region (no disk leakage is considered). The selected boundary conditions and the experimental data are taken from the paper by Moradi *et al.* [14] for rotational speeds of $1500RPM$, $3000RPM$ and $6000RPM$.

A front/rear view of the computational mesh is reported in Figure 7. Five prismatic layers with a grow rate of 1. have been used to model the boundary layer on the viscous walls.

The impeller zone contains $7.8M$ elements while the side channel zone is discretized using $6.7M$ elements. At the maximum flow rate simulated, the average y^+ is about 10. both in the side channel and in the impeller (compatible with the y^+-independent approach used). The numerical results are compared both with the available experimental data and with the numerical data by Moradi *et al.* [14] in Figure 8 and Figure 9. More in detail, the experimental efficiency (here calculated as $\eta = \frac{T_{0,in} - T_{0,out}}{T_{in} - T_{out,is}}$, using the inverse definition for the pump regime) reproduces the total-to-static efficiency shown in [14] whereas the expansion ratio is not directly available from the cited papers and has been recovered using the experimental outlet temperature values. As it can be observed, for the selected working range, there is a very good agreement between the experimental and the numerical efficiency values at $6000RPM$, with discrepancies around 2%. At the other rotational speeds, numerical results match the trend of variation of the efficiency, but the discrepancy increases up to 5%. However, the accuracy of the present computation is close to the one shown in Moradi et al. [14].

Concerning the expansion ratio, the trend of variation is well captured at all the rotational speeds and is very similar to what has been shown in [14]. Still, there is a difference between CFD results and experimental data of ∓ 0.4 at the lower and at the higher flow rate respectively and a difference of -0.1 is found for $0.18kg/s$. Discrepancies increase up to a maximum of $+0.8$ for $0.2kg/s$ at $3000RPM$, with much lower values at other working conditions (i.e., $+0.1$ for $0.10kg/s$ at $1500RPM$). Although the CFD data do not match exactly the performance of the RT, the limited knowledge of the actual working conditions and the improved accuracy of the present data with respect to what is

published in Moradi *et al.* [14] allows for concluding that the numerical method is sufficiently accurate to correctly describe the performance of a regenerative machine in its turbine working range.

For the sake of completeness, the performance of Bartolini's regenerative turbine is also analyzed considering four working conditions in the pump regime. The data reported in Figure 10 show that in the investigated range the compression ratio decreases almost linearly while the efficiency curve increases. As for Yoo's RP, the lack of experimental data does not allow for detailed conclusions; such observations are coherent with what reported in the other sections.

NUMERICAL SIMULATION OF PIERBURG'S RP [10]

The virtual model used for the numerical campaign has already been extensively described by Insinna *et al.* [10] and will only be briefly described here. It consists of a single-sided regenerative pump characterized by semi-circular blades. The Reynolds number of the machine referred to impeller tip velocity and tip diameter is $1.97 \cdot 10^5$. A detailed view of the control volume is reported in Figure 11, whereas a view of the computational mesh can be found in Insinna *et al.* [10]. The overall grid is composed by about 5.6M elements.

Several operating conditions were considered (up to a flow coefficient of 3.5) at different rotational speeds (the design value of $23000RPM$ and two off-design values of $18000RPM$ and $6000RPM$). For all the simulations, flow rate and static pressure were respectively imposed on the inlet and outlet sections. For the calculation of the pressure rise of the machine, the reference sections are in correspondence of the interfaces

between inlet/outlet ducts and porting plate. Performance was also evaluated with the latest version of DART (see Cantini *et al.* [2] for more information) on the operating range of the machine from shut-off conditions to maximum flow rate allowed for the pump.

Results obtained for the Pierburg's RP

The performance of Pierburg's RPaT for the nominal rotational speed of $23000RPM$ over a complete working range (from pump to turbine) is reported in Figure 12. To the best author's knowledge, this is the first time such curve is released in the open literature. The numerical results obtained for the pump are compared with the prediction of the 1D model DART, whereas for the turbine range no reference data are available. It is in the author's opinion that the extensive validation process of the numerical methodology presented in the initial part of the paper supports the validity of the results (at least in a quantitative way).

Figure 12 shows both the load coefficient (negative for the pump regime) and the hydraulic efficiency. For the working region where DART data are available, there is a good agreement between 3D CFD and 1D data except for the fact that DART overestimates the pump efficiency close to the BEP. That kind of behavior is known to the authors and has already been discussed by Insinna *et al.* [10].

The load coefficient increases from negative to positive values changing its sign in a region where the efficiency values are negative (see for example the working point at $\varphi \approx 1.0$). That region represents the theoretical interval $\varphi \in (1-\delta_1, 1+\delta_2)$ obtained from the regenerative machine theory and is approximately limited between $\varphi = 0.8$ and $\varphi = 1.2$. It is interesting to note that the region with negative efficiency starts when the load

coefficient changes it sign, which means that the regenerative machine shows negative efficiency values when it is already working in the turbine range.

Figure 13 reports a detailed view of the load coefficient and efficiency curves for the pump and turbine regimes at different rotational speeds. Figure 13a shows that the agreement of the 1D model with the CFD data decreases when decreasing rotational speeds. Still, the agreement is very good for the nominal value of $23000RPM$ close to the design point ($\varphi \approx 0.5$), which is the aim of the 1D design tool. The efficiency curves (Figure 13c) seem to be slightly affected by the variation of rotational speed, with a variation of 4% at BEP, whereas the 1D model DART greatly overestimates the efficiency over the entire range.

Figure 13b and Figure 13d show the behavior of the Pierburg's pump in the turbine regime. It is interesting to note that the load coefficient does not seem to be affected by the variation of the rotational speed. Furthermore, the load coefficient keeps increasing with the flow coefficient, as already suggested by the data showed in Figure 6 and Figure 8.

Looking at Figure 12, Figure 13b and Figure 13d it is possible to describe the behavior of a RPaT in the turbine region ($\varphi > 1 + \delta_2$). Referring to the figure, for low flow coefficients (approximately $\varphi \in (1 - \delta_1, 1.5)$) the load coefficient increases almost with the same rate shown for the pump working condition whereas the efficiency increases sharply and reaches its maximum value. For higher flow coefficients ($\varphi > 1.5$), the rate of change of the load coefficient increases whereas the efficiency starts to slowly decrease. The fact that the turbine BEP is close to the non-working region could be considered as a negative outcome, but it must be underlined that the efficiency curve for $\varphi > 1.5$ is stable over a

wide range of flow coefficients. That means that it is possible to design a RT that works at a design point which is more stable than the one characterized by the higher efficiency but with limited reduction in the performance. It can be also underlined that the highest efficiency value in the turbine field is much lower (approximately -10%) than the one that characterizes the pump. That outcome seems to be confirmed both by the data obtained for the Yoo's RP in the turbine regime (Figure 6) and by the experimental results by Bartolini and Salvi [13]. Still, more experimental and numerical data in the turbine regime are necessary to determine whether this outcome is confirmed as typical for all the RPaTs or for the considered machine alone.

The map of circulatory velocity characterizing the two working regimes is analyzed in Figure 14 for the $23000RPM$ case. The closer points to the respective BEPs are considered to analyze the circulatory velocity map at the impeller-side channel interface. Black, solid lines represent the zone where the circulatory velocity is zero. As expected, in the pump regime the flow enters the impeller close to the hub while the opposite happens for the turbine regime. The black, dashed lines represent approximately the position of the circulatory pivot in the pump region (based on the radial position where the circulatory velocity changes its sign), this latter being exactly reproduced on the turbine map. As it can be observed, the position of the pivot remains approximately at the same radius, thus suggesting that the assumption that the radial position of the circulatory pivot is governed mainly by geometrical parameters (see [7][10] for more details) is correct both for a RP and a RT. The angular working region is also roughly estimated based on the repetition of a regular pattern for the circulatory velocity. In the pump regime close at BEP the

tangential working region almost include all the portion of machine that goes from the inlet to the outlet channels (green circles in Figure 14); the same cannot be said for the turbine regime where the flow seems to require more space to develop a fully developed circulatory flow. Such an outcome is caused by the fact that the present machine is not perfectly symmetric. In fact, the inlet section is positioned closer to the hub to allow for an improved performance in the pump regime. The same can be said for the outlet section that is positioned at a higher radius. That kind of configuration is not desirable for the turbine range since the flow tends to enter the impeller section at a higher radius. In case of design of a new RPaT, inlet and outlet sections should be positioned both close to the mid-span of the impeller.

To complete the analysis of the flow fields characterizing a RPaT over its complete working range, a slice of the channel of the regenerative machine has been performed in the opposite position with respect to the stripper (where the circulatory flow should be completely developed) for the two flow coefficients close to the BEPs for $23000RPM$. Figure 15 shows the circulatory velocity field over a map that represents the tangential velocity (the rotational velocity being positive with respect to the reported RPaT axis). Tangential velocity maps confirm the inversion of the direction of the helical path between pumps and turbines. Whereas in pumps the flow accelerates in the impeller domain and then recover pressure by decelerating in the side channel, for the turbine the flow in the impeller moves slower than the one in the side channel, coherently with the simplified model shown in Figure 2. The circulatory velocity field furtherly confirms the inversion of the helical path, while it is hard to comment on the actual position of the pivot.

It is also possible to evaluate the adsorbed power (pump) and the net power output (turbine) for the present machine at $23000RPM$. The adsorbed power close to the BEP in the pump region is $\sim 15W$ ($\sim 30W$ at shut-off), which is very close to the corresponding value for the turbine ($\sim 14W$). The net power output for $\varphi > 1.5$ increases up to $170W$ for $\varphi \sim 3.2$. These values are coherent with the purpose of the regenerative pump designed in [10], which is expected to be used as purge pump in the automotive field. However, concerning the usage of a RPaT as a possible tool to recover energy that would be wasted otherwise, it is not straightforward to define a working strategy, but it seems to be clear that, due to the peculiar characteristics of the regenerative machine, the turbine should work at a different (lower) rotational speed for a fixed flow rate to obtain a non-negligible net power output from a fluid stored using the same machine as a pump. A RPaT can be also used either in an air conditioning system to switch from cooling to heating (i.e., in an electrified vehicle) or in a more complex plant where pump and turbine work alternatively in different cycles.

CONCLUSIONS

In the present research activity, the behavior of an existing regenerative pump-as-turbine has been extensively studied using 1D and 3D CFD tools. The existing 1D theory for regenerative pumps has been initially modified to take into consideration also the inverse functioning of a RP. The numerical methodology used for the 3D CFD analysis has been initially validated considering two test cases from the literature (both a RP and a RT). Finally, the performance curve of an existing RP has been extended to include the turbine working region and some comments are provided.

The main conclusions of the research activity follow:

- In regenerative machines, it is possible to switch from pump to turbine by increasing the flow rate only (at a fixed rotational speed). After the switching the helical trajectory changes its direction from clockwise to counterclockwise.
- The position of the circulatory pivot does not change significantly, thus supporting the hypothesis that it depends mainly on geometrical parameters.
- A range of flow coefficients $\varphi \in (1 - \delta_1, 1 + \delta_2)$ where the regenerative machine in not working properly (neither as pump nor as turbine) has been individuated using the 1D model and verified using 3D CFD.
- The not-working region depends on several parameters and affects the turbine range only. In fact, it is caused by a low net power output which is not sufficient to overcome global losses.
- The maximum efficiency obtained in the turbine range seems to be lower than the corresponding value for the pump range (approximately -10% for the studied configuration).
- The net power output of the turbine can be up to ten times higher than the adsorbed power of the pump at the same rotational speed. In principle, it is possible to use a RPaT to store and recover energy considering different rotational speeds for pump and turbine, but also other applications can be explored.

ACKNOWLEDGEMENTS

The authors want to thank sincerely Dr I. S. Yoo (KIMM, Korea Institute of Machinery and Materials) for sharing some details about his work. The authors wish also to thank those listed below for their contribution for without them, this paper would not have been possible: Raffaele Squarcini, Giorgio Peroni and Duccio Griffini (Pierburg Pump Technology Italy SPA), Massimiliano Insinna (CReAI SRL), Alessandro Cappelletti (Enapter), Daniela Anna Misul (Politecnico di Torino), Marco Pierini and Francesco Martelli (Università di Firenze).

NOMENCLATURE

A	Area
C	Coefficients of the V_C equation
g	Gravitational acceleration
H	Pump head
K	Particular solution of the V_C equation
B	Loss coefficient
P	Power (absorbed/produced)
Q	Flow rate
r	Radial coordinate
S	Constant for the calculation of V_C
T	Temperature
U	Impeller speed
V	Velocity

z	Generic function

Greek

α	Incidence factor
β	Blade angle from meridional plane
δ	Support variable
ε	Generic variable
η	Hydraulic efficiency
ϑ	Circulatory efficiency
ϑ	Tangential coordinate
$\varphi = \frac{Q}{Q_s}$	Flow coefficient
Γ	Support variable
σ	Slip factor
$\psi = \frac{gH}{U_{g,0}^2}$	Load coefficient
Ω	Rotational speed

Subscripts

0	Referred to side channel
c	Referred to circulatory trajectory
e	Outlet of the impeller
g	Area centroid
i	Inlet of the impeller
in	Inlet of the machine
is	Isentropic

opt	Optimal
out	Outlet of the machine
s	Referred to solid rotation in the side channel
v	Referred to solid rotation in the impeller vane

REFERENCES

[1] Wilson W. A., Santalo M. A., Oelrich, J. A., 1955, “Theory of the Fluid-Dynamic Mechanism of Regenerative Pumps”, Trans. ASME, Vol. 77, pp. 1303–1316

[2] Cantini G., Salvadori S., Insinna M., Peroni G., Simon G., Griffini D., Squarcini R., 2019, “Development of a One-Dimensional Model for the Prediction of Leakage Flows in Rotating Cavities Under Non-Uniform Tangential Pressure Distribution”, Int. J. Turbomach. Propuls. Power, Vol. 4, Issue 3, No. 19, doi: 10.3390/ijtpp4030019

[3] Karassik I. J., Messina J. P., Cooper P., Heald C. C., 2001, “Pump Handbook”. McGraw-Hill, 2001, ISBN:0070340323

[4] Brown A., 1972, “A Comparison of Regenerative and Centrifugal Compressors”, International Compressor Engineering Conference, Paper No. 34

[5] Sixsmith H., Altmann H., 1977, “A Regenerative Compressor”, Journal of Engineering for Industry, Vol. 99, Issue 3, pp. 637-647, doi: 10.1115/1.3439291

[6] Griffini D., Salvadori S., Carnevale M., Cappelletti A., Ottanelli L., Martelli F., 2015, “On the Development of an Efficient Regenerative Compressor”, Energy Procedia, Vol. 82, pp. 252-257, doi: 10.1016/j.egypro.2015.12.030

[7] Yoo I. S., Park M. R., Chung M. K., 2005, “Improved Momentum Exchange Theory for Incompressible Regenerative Turbomachines”, Proceedings of the Institution of

Mechanical Engineers, Part A: Journal of Power and Energy, Vol. 219, Issue 7, pp: 567–581, doi: 10.1243/095765005X31252

[8] Yoo I. S., Park M. R., Chung M. K., 2006, “Hydraulic design of a regenerative flow pump for an artificial heart pump”, Proceedings of the Institution of Mechanical Engineers, Part A: Journal of Power and Energy, Vol. 220, Issue 7, pp. 699–706, doi: 10.1243/09576509JPE211

[9] Badami M., Mura, M., 2010, “Theoretical Model with Experimental Validation of a Regenerative Blower for Hydrogen Recirculation in a PEM Fuel Cell System”, Energy Conversion and Management, Vol. 51, Issue 3, pp. 553-560

[10] Insinna M., Salvadori S., Martelli F., Peroni G., Simon G., Dipace A., Squarcini R., 2018, “One-Dimensional Prediction and Three-Dimensional CFD Simulation of the Fluid Dynamics of Regenerative Pumps”, Proc. of the ASME Turbo Expo 2018, Vol. 2C, V02CT42A036, Lillestrøm, Norway, June 11-15, doi: 10.1115/GT2018-76416, Paper No. GT2018-76416

[11] Baljé O. E., 1957, “Drag Turbine Performance”, ASME Paper 56-AV

[12] Baljé O. E., 1981. “Turbomachines – A Guide to Design Selection and Theory”, Wiley-Interscience, New York, 1981, 528 pp.

[13] Bartolini C. M., Salvi D., 1996, “Experimental Analysis of a Small Prototype of Peripheral Turbine for Decompression of Natural Gas”, Proc. of the ASME 1996 International Gas Turbine and Aeroengine Congress and Exhibition, Vol. 3, V003T07A015, Birmingham, UK, June 10–13, doi: 10.1115/96-GT-515, Paper No. 96-GT-515

[14] Moradi R., Cioccolanti L., Bocci E., Villarini M., Renzi M., 2019, “Numerical Investigation on the Performance of a Regenerative Flow Turbine for Small-Scale Organic Rankine Cycle Systems”, Journal of Engineering for Gas Turbines and Power, Vol. 141, Issue 9, doi: 10.1115/1.4044062

[15] Salvadori S., Marini A., Martelli F., 2012, “Methodology for the Residual Axial Thrust Evaluation in Multistage Centrifugal Pumps”, Engineering Applications of Computational Fluid Mechanics, Vol. 6, Issue 2, pp. 271-284, doi: 10.1080/19942060.2012.11015420

[16] Bontempo R., Manna M., 2016, “Analysis and “Evaluation of the Momentum Theory Errors as Applied to Propellers”, AIAA Journal, Vol. 54, Issue 12, pp. 3840-3848

[17] Griffini D., Salvadori S., Martelli F., 2016, “Thermo-Hydrodynamic Analysis of Plain and Tilting Pad Bearings”, Energy Procedia, Vol. 101, pp. 2-9, doi: 10.1016/j.egypro.2016.11.001

[18] Yoo I. S., personal communication

[19] Quail F., Scanlon T., Stickland M., 2011, “Design Optimisation of a Regenerative Pump using Numerical and Experimental Techniques”, International Journal of Numerical Methods for Heat & Fluid Flow, Vol. 21, Issue 1, pp: 95-111, doi: 10.1108/09615531111095094

[20] Nejadrajabali J., Riasi A., Nourbakhsh S. A., 2016, “Flow Pattern Analysis and Performance Improvement of Regenerative Flow Pump using Blade Geometry Modification”, International Journal of Rotating Machinery, Vol. 2016, Article ID 8628467, doi:10.1155/2016/8628467

[21] Shih T.-H., Liou W. W., Shabbir A., Yang Z., Zhu J., 1995, “A New k-ε Eddy-Viscosity Model for High Reynolds Number Turbulent Flows - Model Development and Validation”, Computers & Fluids, Vol. 24, No. 3, pp: 227–238, doi: 10.1016/0045-7930(94)00032-T

[22] ANSYS® Fluent® Theory Guide, Release 19.4. 2019

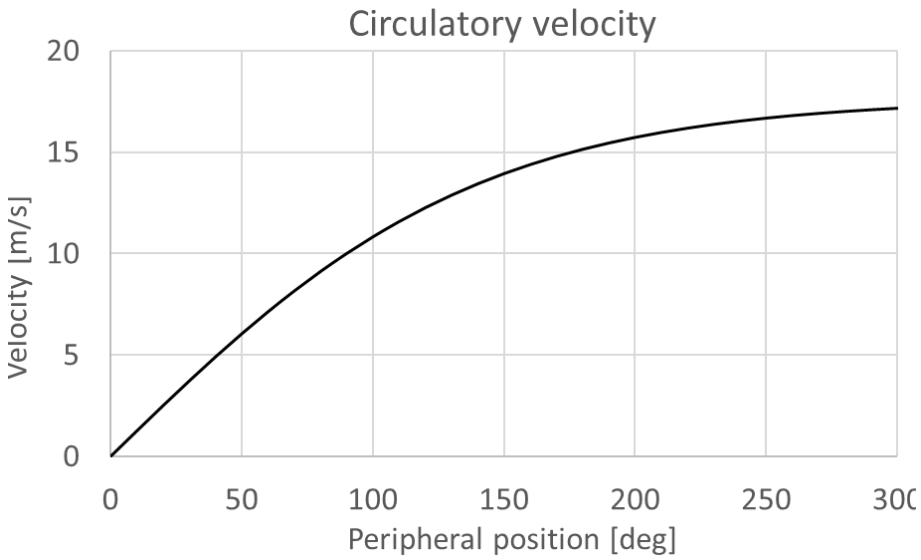

Figure 1: Circulatory velocity pattern as a function of the peripheral coordinate

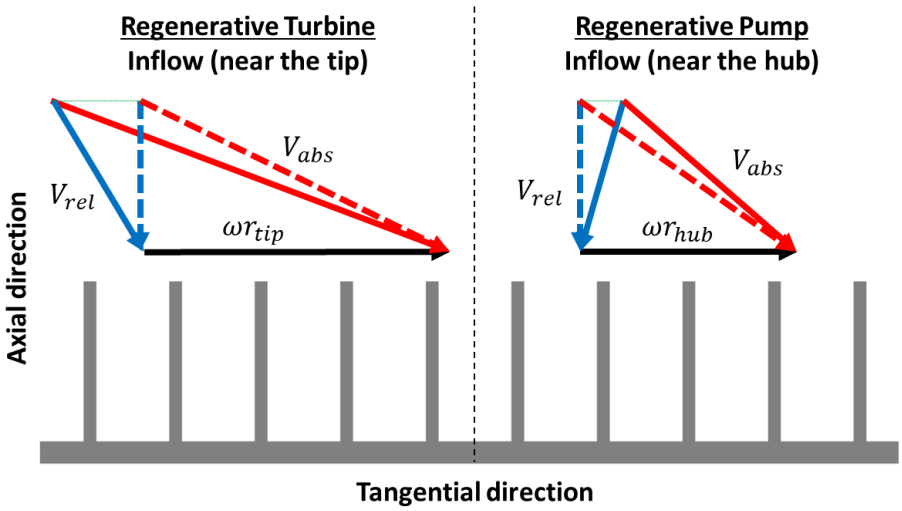

Figure 2: Velocity triangles for a RT and a RP

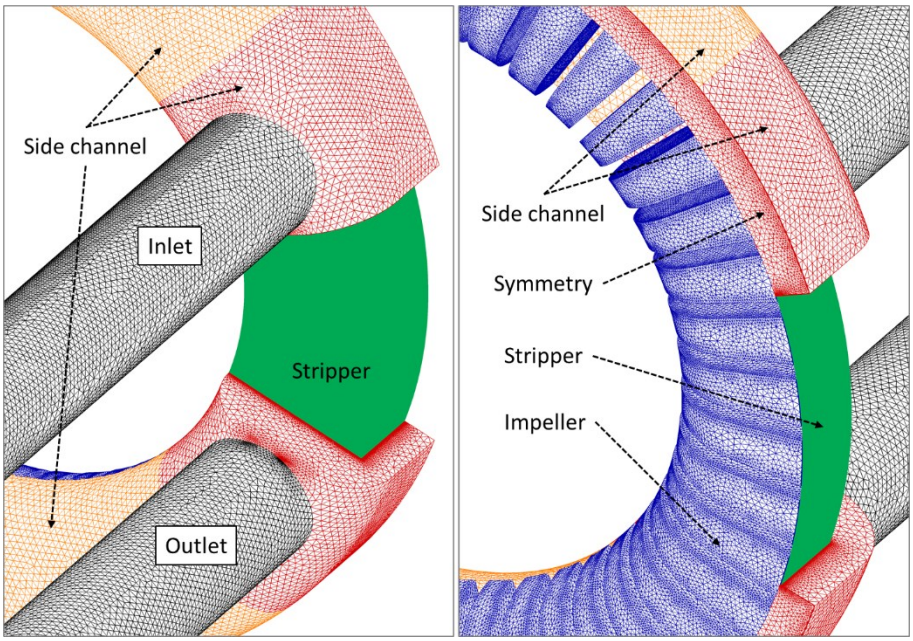

Figure 3: Computational mesh for Yoo's RP [7]

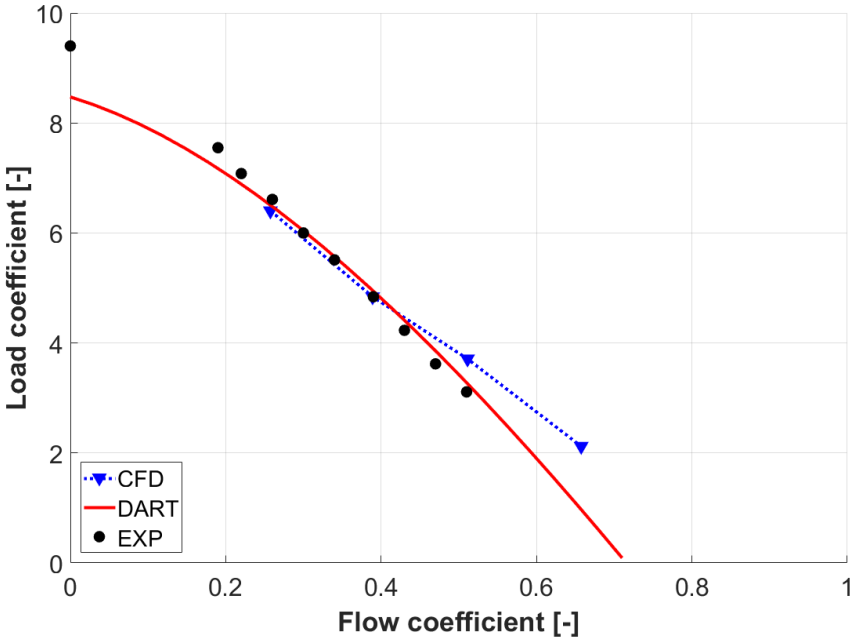

Figure 4: Load coefficient of Yoo's RP [7]

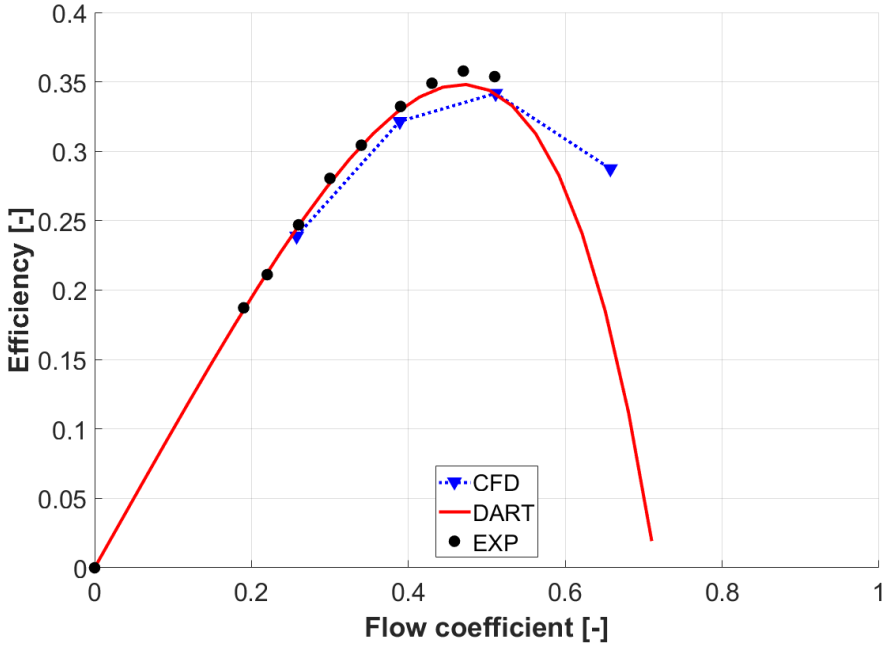

Figure 5: Efficiency of Yoo's RP [7]

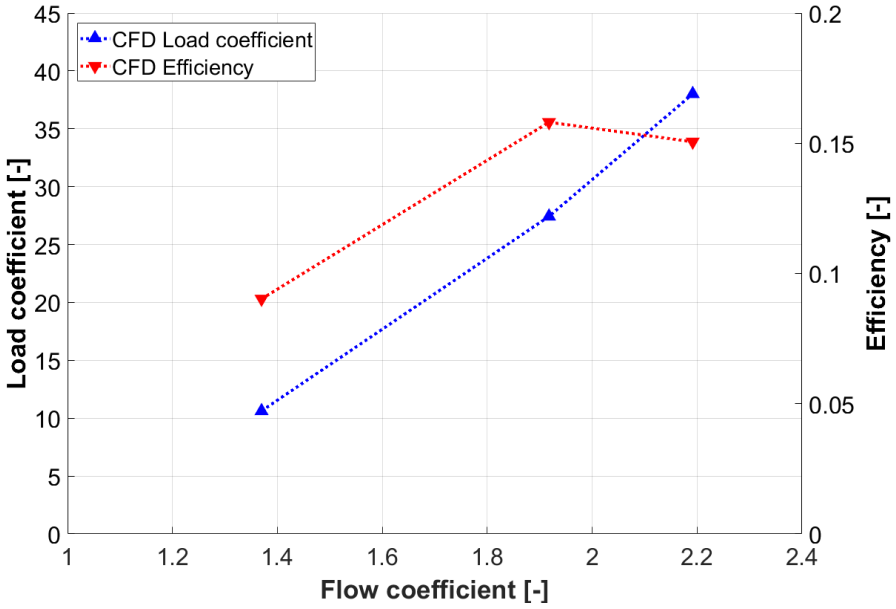

Figure 6: Performance curves of Yoo's RT

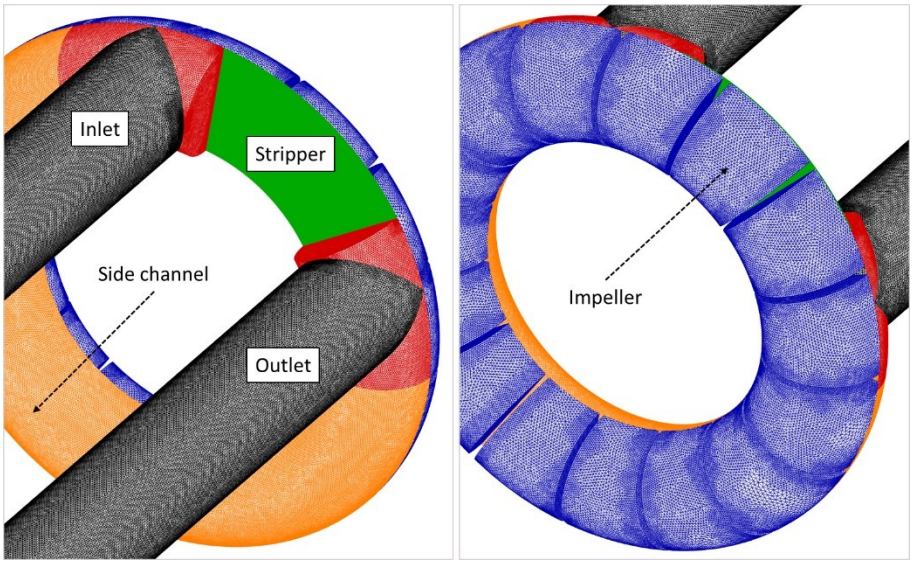

Figure 7: Computational mesh for Bartolini's RT [13]

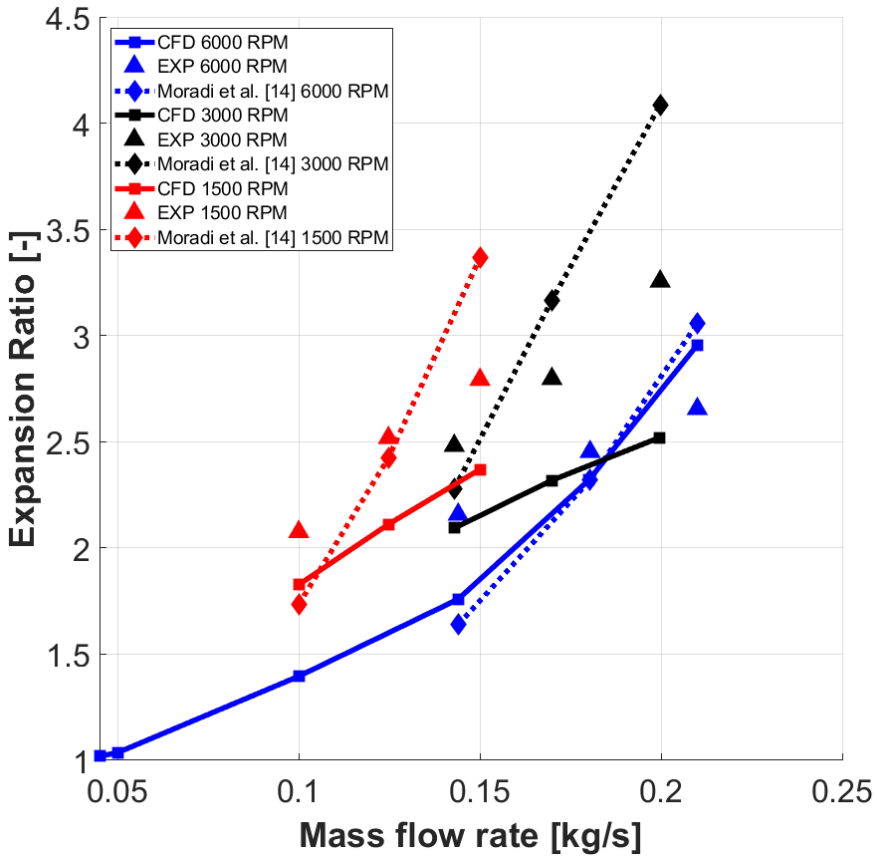

Figure 8: Expansion ratio of Bartolini's RT [13][14]

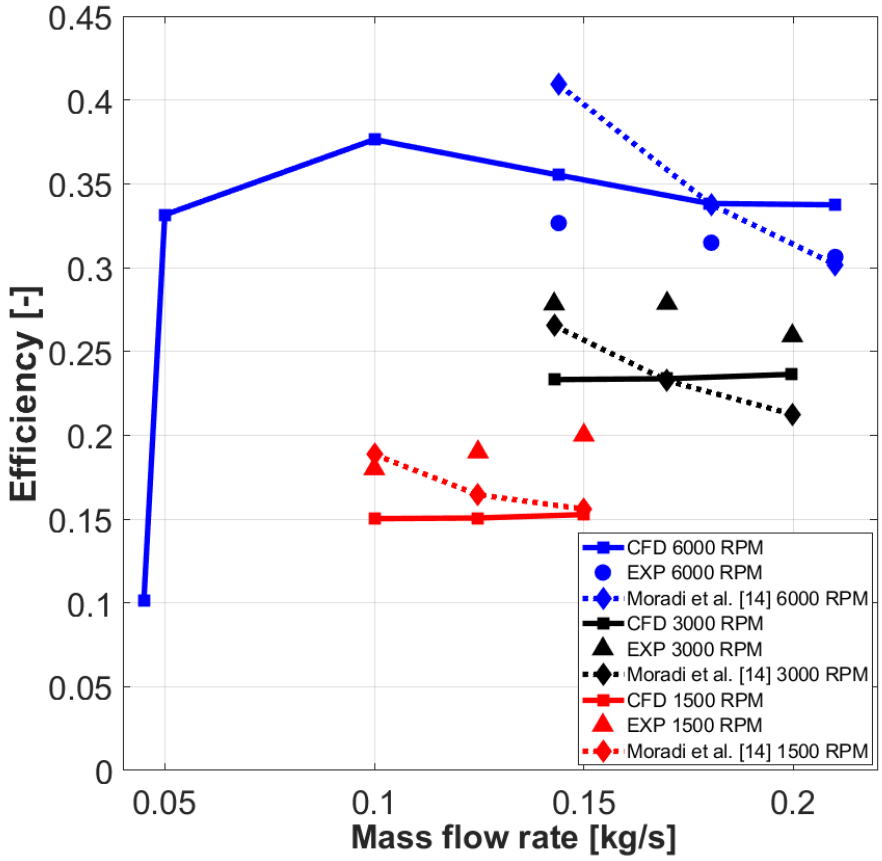

Figure 9: Efficiency of Bartolini's RT [13][14]

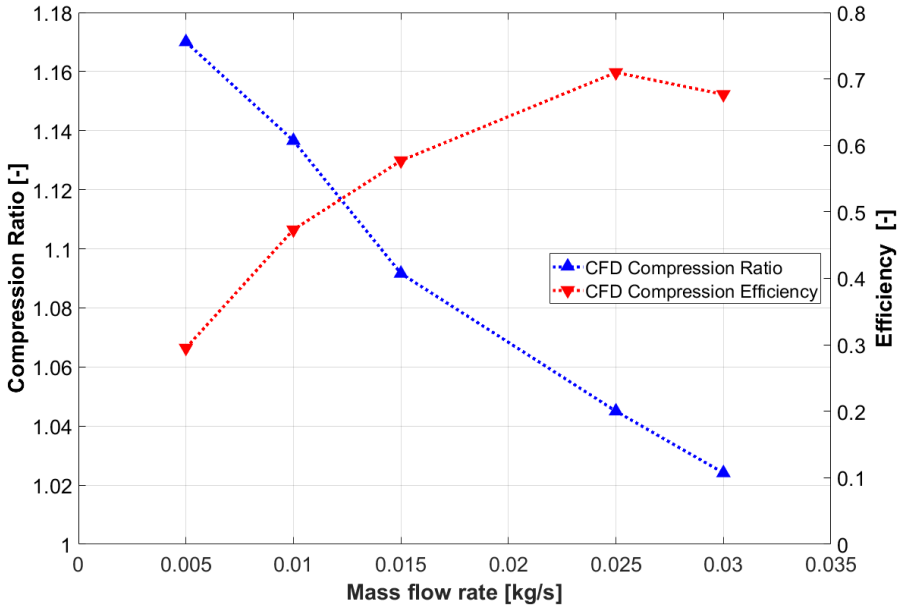

Figure 10: Compression ratio of Bartolini's RP

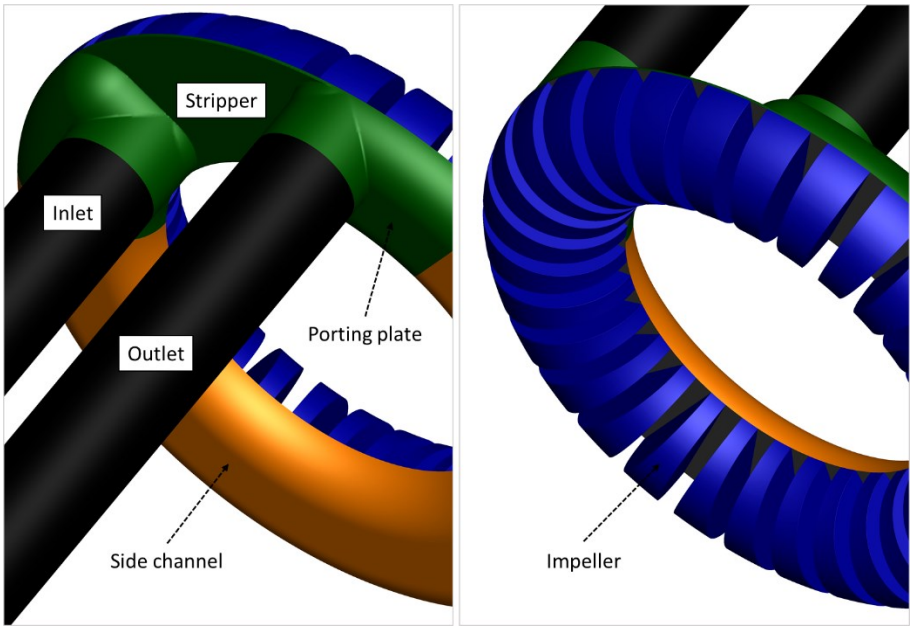

Figure 11: Computational domain of the Pierburg's RPaT [10]

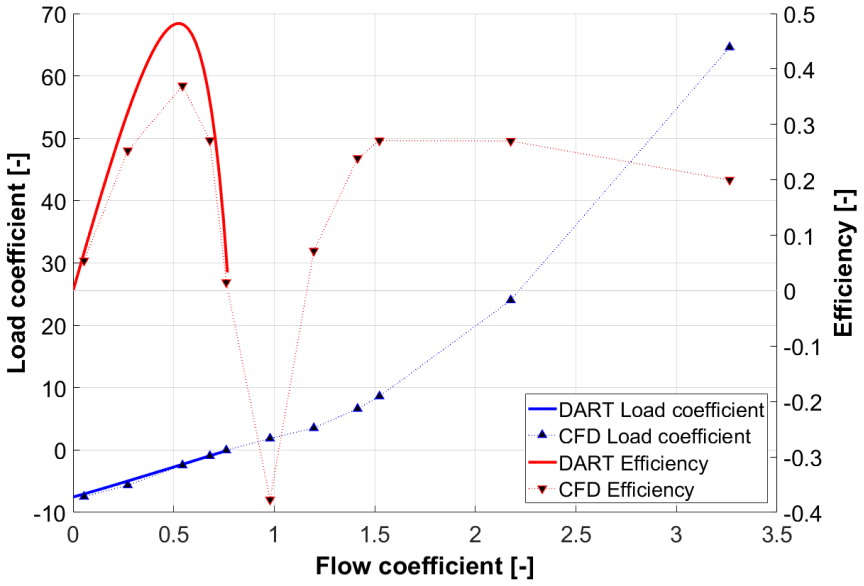

Figure 12: RPaT performance curves for $\Omega = 23000RPM$

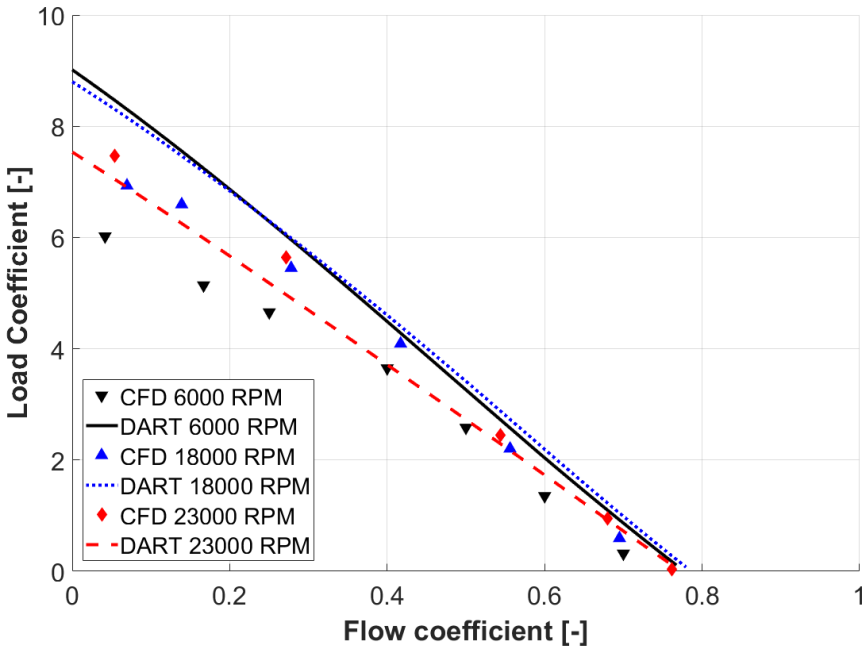

Figure 13: (a) Load coefficient of Pierburg's RP

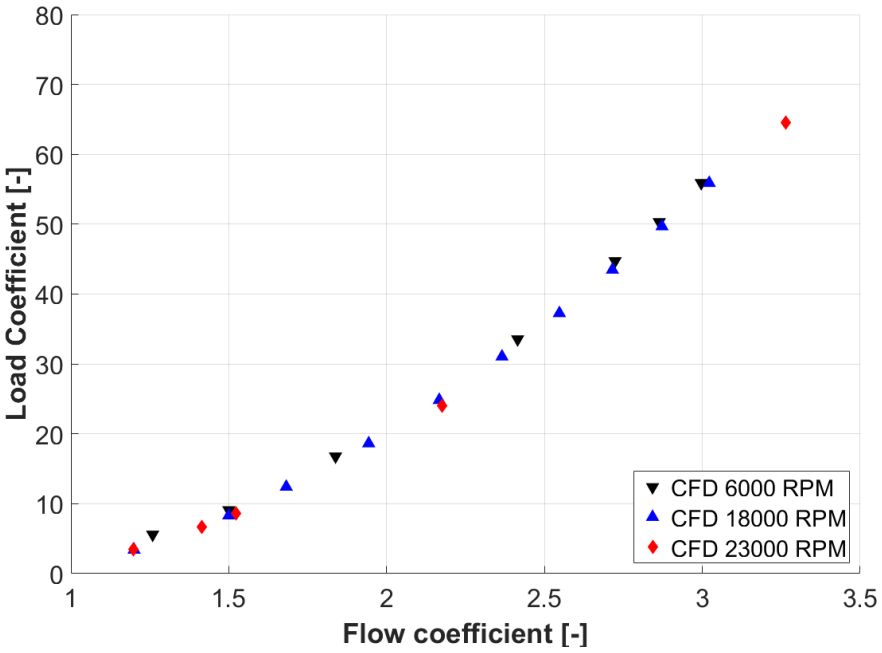

Figure 13: (b) Load coefficient of Pierburg's RT

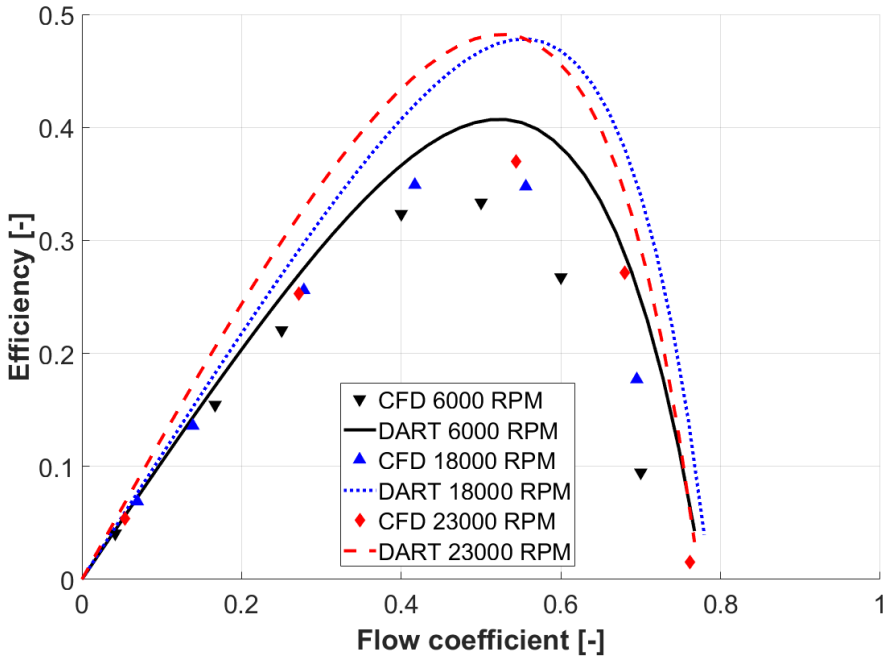

Figure 13: (c) Efficiency of Pierburg's RP

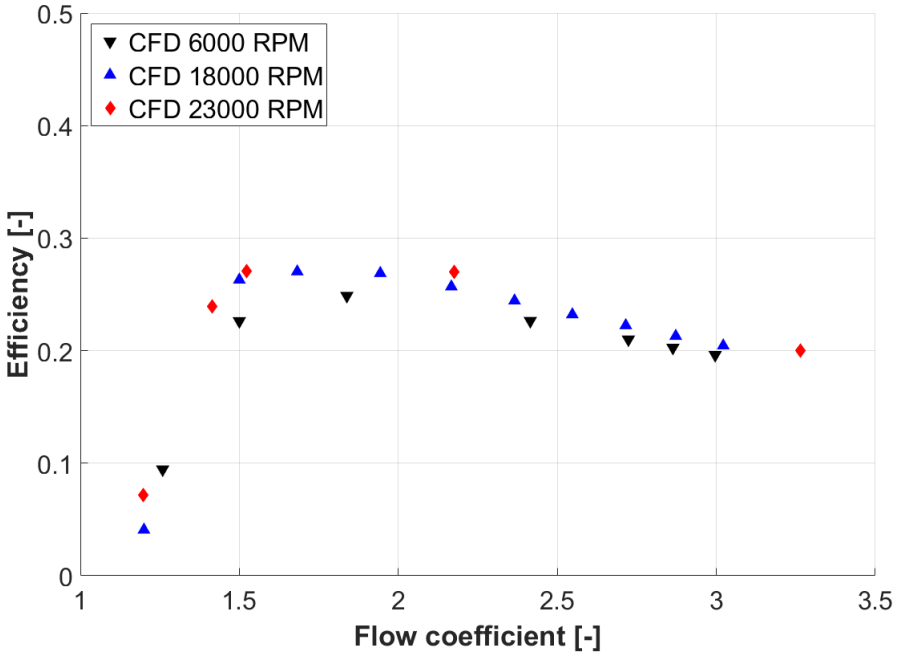

Figure 13: (d) Efficiency of Pierburg's RT

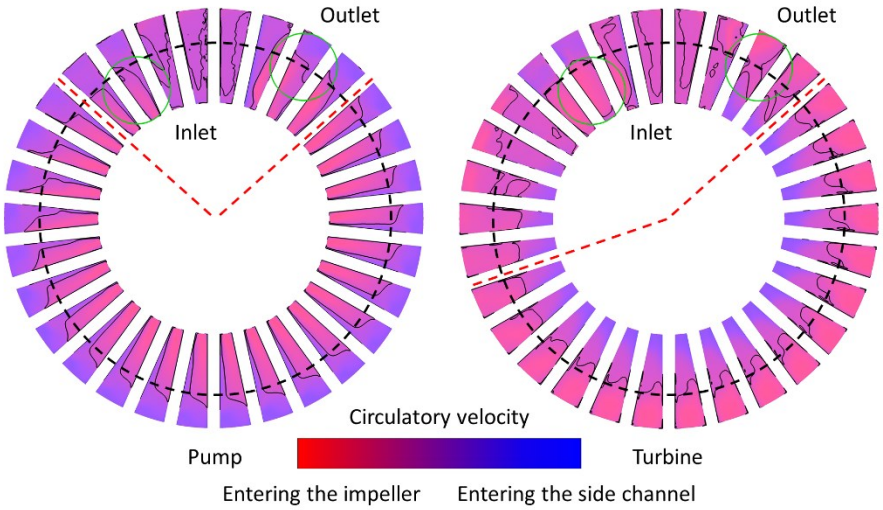

Figure 14: Maps of the circulatory velocity with the approximate position of the circulatory pivot and estimated working section

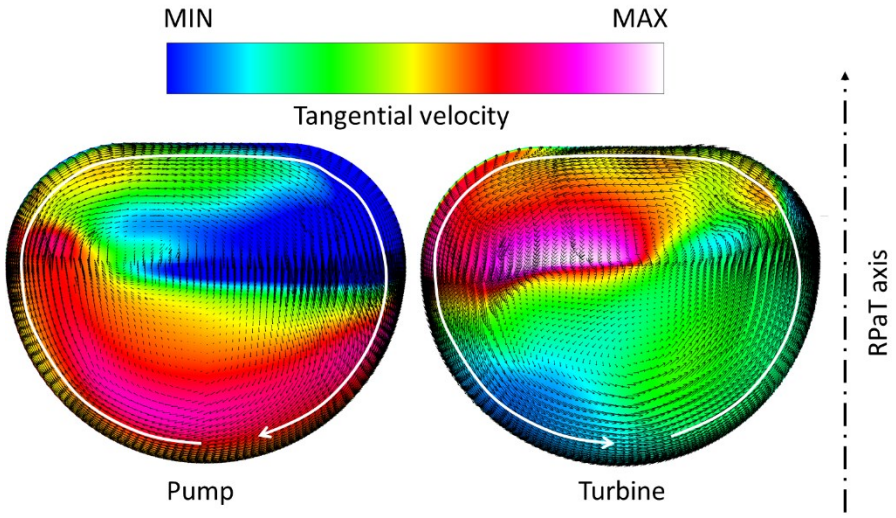

Figure 15: Circulatory velocity flow field with maps of tangential velocity inside of a impeller vane and side channel